

## REPORT No. 888

### A THEORY OF UNSTAGGERED AIRFOIL CASCADES IN COMPRESSIBLE FLOW

By ROBERT A. SPURR and H. JULIAN ALLEN

#### SUMMARY

By use of the methods of thin airfoil theory, which include effects of compressibility, relations are developed which permit the rapid determination of the pressure distribution over an unstaggered cascade of airfoils of a given profile, and the determination of the profile shape necessary to yield a given pressure distribution for small chord/gap ratios. For incompressible flow the results of the theory are compared with available examples obtained by the more exact method of conformal transformation. Although the theory is developed for small chord/gap ratios, these comparisons show that it may be extended to chord/gap ratios of order unity, at least for low-speed flows. Choking of cascades, a phenomenon of particular importance in compressor design, is considered.

#### INTRODUCTION

The wider use of gas turbines and other devices employing axial-flow compressors has increased the need for compressors with a high pressure rise per stage. In order to achieve this purpose it is necessary to use high velocity flows, thus increasing the possibility of losses through compression shock. A method is therefore desirable which will permit the design of compressor blades which have high critical compressibility speeds. This result can be accomplished if a cascade of airfoils representing the flow can be designed to give a desirable airfoil-section pressure distribution.

This report attacks a portion of the problem by finding the relation between the profile shape and pressure distribution over airfoils arranged in an unstaggered cascade through the use of the approximate methods of thin airfoil theory originally presented by Glauert in reference 1 and further developed by the NACA in reference 2. The flow over an airfoil in cascade is related to that over a single airfoil in a free stream. The problem of finding the pressure distribution over an airfoil in cascade or the shape of an airfoil in cascade to give a required pressure distribution then reduces to the analogous problem for a single airfoil, which can be solved by known methods.

The analysis involves the assumption that the gap between airfoils is large compared to the chord length. In particular, expressions relating the characteristics of a cascade airfoil to those of a free airfoil are expanded in a power series in  $c/g$ , where  $c$  is the chord and  $g$  the perpendicular distance between airfoil chord lines in the cascade, and powers of  $c/g$  higher

than the second are neglected. Definitions of the symbols used are found in Appendix A.

#### THEORY

Consider an infinite unstaggered cascade of identical two-dimensional airfoils, as represented in figure 1. The configuration is specified by the chord/gap ratio  $c/g$ , the camber-line shape and thickness distribution of the individual airfoils. For an individual airfoil, the incident velocity is  $V$  with a corresponding density of  $\rho$  and angle of attack  $\alpha'$ .

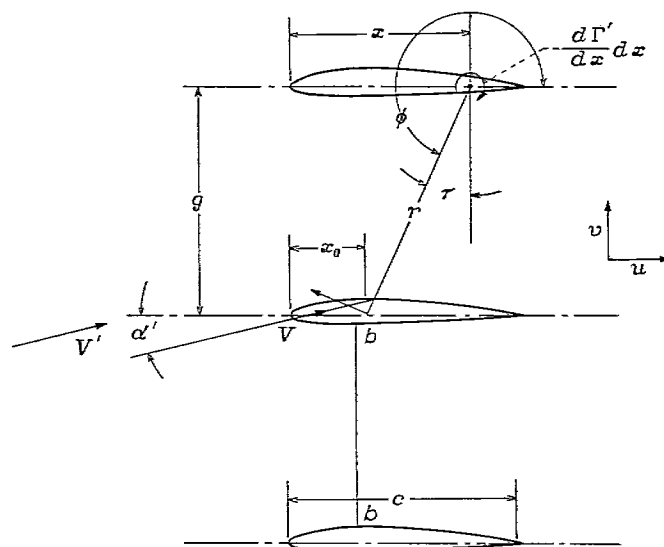


FIGURE 1.—Schematic diagram of cascade.

The pressure distribution on a typical cascade airfoil will be compared with that which would be obtained over a single airfoil of the same shape in a stream of velocity  $V$  and density  $\rho$ . The angle of attack  $\alpha$  of the single airfoil will not, in general, be the same as the angle of attack  $\alpha'$  of the airfoil in cascade, and an expression relating the two angles will be given. In the analysis to follow, primes will be used to designate properties of the cascade airfoil.

#### AERODYNAMIC CHARACTERISTICS OF A CASCADE AIRFOIL OF A GIVEN PROFILE SHAPE

Effect of camber.—The chordwise lift distribution for the free airfoil is given by the Kutta-Joukowski relation

$$\frac{dL}{dx} = \rho V \frac{d\Gamma}{dx} \quad (1)$$

where  $L$  is lift per unit span,  $\Gamma$  is the vorticity per unit span, and  $x$  is the chordwise distance from the leading edge to the point in question. The lift-distribution coefficient  $P$  is then defined as

$$P = \frac{1}{q} \frac{dL}{dx} = \frac{2}{V} \frac{d\Gamma}{dx} \quad (2)$$

In Appendix B, it is shown that the stream velocity at the cascade airfoil is uniform so that the lift distribution for the cascade airfoil may be expressed as

$$\frac{dL'}{dx} = \rho V \frac{d\Gamma'}{dx} \quad (3)$$

and the lift-distribution coefficient of the cascade airfoil referred to the dynamic pressure  $q$  is

$$P^* = \frac{1}{q} \frac{dL'}{dx} = \frac{2}{V} \frac{d\Gamma'}{dx} \quad (4)$$

From equations (2) and (4),

$$P^* - P = \frac{2}{V} \left( \frac{d\Gamma'}{dx} - \frac{d\Gamma}{dx} \right) \quad (5)$$

It is now desirable to express equation (5) in a more convenient form. It is assumed that the vorticity distributions of the free and cascade airfoils, respectively, may be represented by the following series (references 1 and 2):

$$\left. \begin{aligned} \frac{d\Gamma}{dx} &= 2V \left( A_0 \cot \frac{1}{2} \theta + \sum_{n=1}^{\infty} A_n \sin n\theta \right) \\ \frac{d\Gamma'}{dx} &= 2V \left( A_0' \cot \frac{1}{2} \theta + \sum_{n=1}^{\infty} A_n' \sin n\theta \right) \end{aligned} \right\} \quad (6)$$

The new parameter  $\theta$  is related to  $x$  by the equation

$$x = \frac{c}{2} (1 - \cos \theta) \quad (7)$$

Equation (5) then becomes

$$P^* - P = 4 \left[ (A_0' - A_0) \cot \frac{1}{2} \theta + \sum_{n=1}^{\infty} (A_n' - A_n) \sin n\theta \right] \quad (8)$$

The coefficients in equation (8) will now be evaluated by considering the conditions of flow at the airfoil boundaries. Let  $v$  and  $v'$  be the vertical components of velocity induced, respectively, by the free airfoil and a particular cascade airfoil, and let  $\Delta v$  be the vertical component of velocity induced by the other airfoils of the cascade. For small angles of attack, in order that the flow be tangent at the surfaces, the slope  $dy_c/dx$  of the airfoil camber line (which is the same for both free and cascade airfoils) must be given by the following relations:

$$\left. \begin{aligned} \frac{dy_c}{dx} &= \alpha + \frac{v}{V} \\ \frac{dy_c}{dx} &= \alpha' + \frac{v'}{V} + \frac{\Delta v}{V} \end{aligned} \right\} \quad (9)$$

Appendix B gives the vertical components of velocity induced by the vorticity and source-sink distributions which represent the airfoils of a cascade. For simplicity, the following symbols are used:

$$\sigma = \frac{\pi^2 c^2}{48 g^2} \quad (B11)$$

$$\lambda = \sqrt{1 - M^2} \quad (B4)$$

where  $M$  is the Mach number of the undisturbed stream.

The velocity components calculated in Appendix B are

$$\frac{v}{V} = \lambda \left( -A_0 + \sum_{n=1}^{\infty} A_n \cos n\theta \right) \quad (B5)$$

$$\frac{v'}{V} = \lambda \left( -A_0' + \sum_{n=1}^{\infty} A_n' \cos n\theta \right) \quad (B6)$$

and neglecting terms involving  $\sigma$  to the second and higher powers

$$\frac{\Delta v}{V} = -2 \frac{\sigma}{\lambda} \left[ (A_0' + \frac{1}{2} A_2') - (2A_0' + A_1') \cos \theta \right] \quad (B25)$$

Substituting these relations in equations (9), there is obtained

$$\left. \begin{aligned} \frac{dy_c}{dx} &= \alpha + \lambda \left( -A_0 + \sum_{n=1}^{\infty} A_n \cos n\theta \right) \\ \frac{dy_c}{dx} &= \alpha' + \lambda \left( -A_0' + \sum_{n=1}^{\infty} A_n' \cos n\theta \right) \\ &\quad - 2 \frac{\sigma}{\lambda} \left[ (A_0' + \frac{1}{2} A_2') - (2A_0' + A_1') \cos \theta \right] \end{aligned} \right\} \quad (10)$$

Since equations (10) are equal trigonometric series, the coefficients of  $\cos n\theta$  can be equated:

$$\left. \begin{aligned} \alpha - \lambda A_0 &= \alpha' - \lambda A_0' - 2 \frac{\sigma}{\lambda} (A_0' + \frac{1}{2} A_2') \\ \lambda A_1 &= \lambda A_1' + 2 \frac{\sigma}{\lambda} (2A_0' + A_1') \\ A_2 &= A_2' \\ &\dots \dots \dots \\ A_n &= A_n' \quad (n \neq 1) \end{aligned} \right\} \quad (11)$$

From the first of equations (11), it is seen that the quantity  $(A_0' - A_0)$  depends on the angle of attack  $\alpha$  of the free airfoil. This angle may be arbitrarily defined so that

$$A_0' - A_0 = 0 \quad (12)$$

Combining equations (11) and (12), the following relations are obtained:

$$\left. \begin{aligned} A_1' - A_1 &= 0 \\ A_1' - A_1 &= -2 \frac{\sigma}{\lambda^2} (2A_0' + A_1') \\ A_2' - A_2 &= 0 \\ &\dots \dots \dots \\ A_n' - A_n &= 0 \quad (n \neq 1) \end{aligned} \right\} \quad (13)$$

and

$$\alpha' - \alpha = 2 \frac{\sigma}{\lambda} \left( A_0' + \frac{1}{2} A_2' \right) \quad (14)$$

Making use of equations (13), equation (14) may also be written as follows:

$$\alpha' - \alpha = 2 \frac{\sigma}{\lambda} \left( A_0 + \frac{1}{2} A_2 \right) \quad (15)$$

From equations (8) and (13), there is obtained

$$P^* - P = -8 \frac{\sigma}{\lambda^2} (2A_0' + A_1') \sin \theta \quad (16)$$

Changing to the unprimed coefficients with the use of equations (13), and neglecting terms in  $\sigma^2$ , the expression becomes

$$P^* - P = -8 \frac{\sigma}{\lambda^2} (2A_0 + A_1) \sin \theta \quad (17)$$

It should not be interpreted from equations (16) and (17) that  $A_1'$  and  $A_1$  are equal. Equation (17) is the result of dropping terms in  $\sigma^2$  and not of equating  $A_1'$  and  $A_1$ . The difference between  $A_1'$  and  $A_1$  to the order  $\sigma$  is still given by equations (13).

The section lift coefficient for the free airfoil is

$$c_l = \int_0^1 P d \left( \frac{x}{c} \right) \quad (18)$$

Substituting from equations (2), (6), and (7) and performing the integration, one obtains

$$c_l = \pi (2A_0 + A_1) \quad (19)$$

Similarly, the quarter-chord moment coefficient is

$$c_{m_{c/4}} = \int_0^1 P \left( \frac{1}{4} - \frac{x}{c} \right) d \left( \frac{x}{c} \right) = -\frac{\pi}{4} (A_1 - A_2) \quad (20)$$

From equations (19) and (20) it follows that

$$\left. \begin{aligned} 2A_0 + A_1 &= \frac{c_l}{\pi} \\ A_0 + \frac{1}{2} A_2 &= \frac{1}{2\pi} (c_l + 4c_{m_{c/4}}) \end{aligned} \right\} \quad (21)$$

With use of equations (21), equations (15) and (17) then become

$$\alpha' - \alpha = \frac{\sigma}{\pi \lambda} \left( c_l + 4c_{m_{c/4}} \right) \quad (22)$$

and

$$P^* - P = -\frac{8\sigma c_l}{\pi \lambda^2} \sin \theta \quad (23)$$

$$= -\frac{16\sigma c_l}{\pi \lambda^2} \sqrt{\frac{x}{c} \left( 1 - \frac{x}{c} \right)} \quad (24)$$

**Effect of thickness.**—From Appendix B, the horizontal velocity at an airfoil in cascade is greater than that at a single airfoil by the amount  $\Delta u$ , which is given by the relation

$$\frac{\Delta u}{V} = \frac{\Delta \sigma}{\lambda^3} \quad (B24)$$

The quantity  $\Delta$  is a function of airfoil thickness given by equation (B20) and tabulated for various airfoils in table I, which has been taken from reference 3.

The increment of velocity given by equation (B24) can be added to the velocity of the undisturbed stream  $V_1$  to give the true incident velocity  $V$ :

$$V = V_1 + \Delta u \quad (25)$$

From equations (B24) and (25),

$$\frac{V_1}{V} = 1 - \frac{\Delta \sigma}{\lambda^3} \quad (26)$$

The density  $\rho_1$  far ahead of the cascade is given by the following equation, derived for isentropic flow:

$$\rho_1 = \rho \left\{ 1 - \frac{\gamma-1}{2} M^2 \left[ \left( \frac{V_1}{V} \right)^2 - 1 \right] \right\}^{\frac{1}{\gamma-1}}$$

where  $\gamma$  is the ratio of specific heat at constant pressure to that at constant volume. Using the binomial expansion and neglecting terms containing powers of  $[(V_1/V)^2 - 1]$  higher than the first, there is obtained to the order of  $\sigma$

$$\frac{\rho_1}{\rho} = 1 + \frac{\Delta \sigma M^2}{\lambda^3} \quad (27)$$

The ratio of the dynamic pressure  $q$  at the center of pressure to the dynamic pressure  $q_1$  far ahead of the airfoil is then found to be

$$\frac{q}{q_1} = 1 + 2 \frac{\Delta \sigma \xi}{\lambda^3} \quad (28)$$

where

$$\xi = 1 - \frac{M^2}{2} \quad (29)$$

The lift-distribution coefficient  $P'$  referred to the dynamic pressure  $q_1$  is given by

$$P' = \frac{q}{q_1} P^* \quad (30)$$

The cascade section lift coefficient is

$$c_l' = \int_0^1 P' d \left( \frac{x}{c} \right) = \frac{q}{q_1} \int_0^1 P^* d \left( \frac{x}{c} \right) \quad (31)$$

Substituting equations (24) and (28) in equation (31) and performing the integration, there is obtained, neglecting terms in  $\sigma^2$ ,

$$c_l' - c_l = -2 \frac{\sigma c_l}{\lambda^2} \left( 1 - \frac{\xi \Delta}{\lambda} \right) \quad (32)$$

Equation (32) gives the relation between the lift coefficient of a cascade airfoil at angle of attack  $\alpha'$  and that of a single airfoil at angle of attack  $\alpha$ . The relation between  $\alpha'$  and  $\alpha$  is given by equation (22).

The Mach number  $M'$  must now be related to the Mach number  $M$  for the corresponding single airfoil. The velocity of sound  $a_1$  is related to  $a$  by

$$a_1 = \sqrt{\frac{T_1}{T}} a \quad (33)$$

For isentropic flow

$$T_1 = T \left\{ 1 - \frac{\gamma-1}{2} M^2 \left[ \left( \frac{V_1}{V} \right)^2 - 1 \right] \right\}$$

which becomes, using equation (26)

$$T_1 = T \left[ 1 + (\gamma-1) M^2 \frac{\Delta\sigma}{\lambda^3} \right] \quad (34)$$

Hence equation (33) becomes, to the order of  $\sigma$

$$a_1 = \left( 1 + \frac{\gamma-1}{2} M^2 \frac{\Delta\sigma}{\lambda^3} \right) a \quad (35)$$

and so

$$M' = \frac{V_1}{a_1} = \left( \frac{V_1}{V} \right) \frac{a}{a_1} M$$

Using equations (26) and (35) then

$$M' = \left( 1 - \frac{\Delta\sigma}{\lambda^3} \mu \right) M \quad (36)$$

where

$$\mu = 1 + \left( \frac{\gamma-1}{2} \right) M^2 \quad (37)$$

**Determination of pressure coefficient.**—The following coefficients are useful in expressing the pressure on an airfoil surface:

$$S_l = \frac{H-p_l}{q}; P_l = \frac{p_l-p}{q} \quad (38)$$

where  $p_l$  is the local static pressure on the surface of the airfoil, and  $H$ ,  $p$ , and  $q$  are, respectively, the total head, static pressure, and dynamic pressure of the undisturbed stream. The variation of  $H$  with Mach number, assuming that the ratio of specific heats is 1.4, is given (reference 4) by the equations

$$\left. \begin{aligned} H &= p + q(1+\eta) \\ 1+\eta &= 1 + \frac{M^2}{4} + \frac{M^4}{40} + \frac{M^6}{1600} + \dots \end{aligned} \right\} \quad (39)$$

From these equations,

$$S_l = 1 + \eta - P_l \quad (40)$$

A graph of  $\eta$  as a function of Mach number is given in figure 2. The subscript  $l$  in equations (38) and (40) will be replaced by  $U$ ,  $L$ , or  $f$  to denote, respectively, the upper and lower surfaces of an airfoil and the surface of its symmetrical base profile.

According to reference 5, the velocity  $V_f$  along the base profile of a single airfoil is given for incompressible flow by the expression

$$\frac{V_f}{V} = \sqrt{1-P_f} = \frac{\sqrt{1-P_U} + \sqrt{1-P_L}}{2} \quad (41)$$

where the pressure coefficients are referred to  $q$ . That is,

$$P_U = \frac{p_U-p}{q}; P_L = \frac{p_L-p}{q}; P_f = \frac{p_f-p}{q}$$

and  $p$  is the static pressure of the stream corresponding to  $q$ .

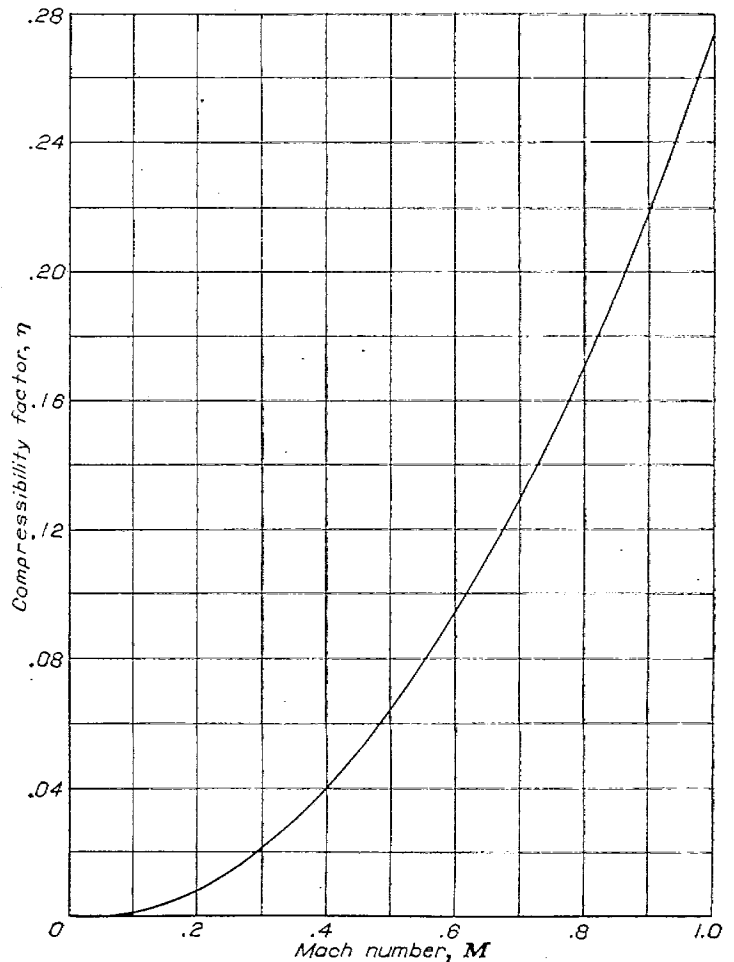


FIGURE 2.—Compressibility factor,  $\eta$ , as a function of Mach number.

The velocity  $V_f'$  along the base profile of the airfoil in a cascade in terms of  $V$  is simply

$$\frac{V_f'}{V} = \frac{V_f}{V}$$

so that

$$\sqrt{1-P_f'^*} = \sqrt{1-P_f} \quad (42)$$

since the cascade base-profile pressure coefficient  $P_f'^*$  is referred to the dynamic pressure  $q$  and to the static pressure  $p$  rather than to the corresponding quantities in the undisturbed stream. Analysis (reference 3) shows that equation (42) holds also for compressible flow, to an approximation of the same order of magnitude as others already made.

The upper- and lower-surface pressure coefficients referred to  $q$  are from reference 5.

$$\left. \begin{aligned} P_U^* &= 1 - \frac{\left( 1 - P_f^* + \frac{1}{4} P^* \right)^2}{1 - P_f^*} \\ P_L^* &= 1 - \frac{\left( 1 - P_f^* - \frac{1}{4} P^* \right)^2}{1 - P_f^*} \end{aligned} \right\} \quad (43)$$

Although equations (43) were derived for incompressible flow, it can be shown that they are applicable in the case of flow in a compressible stream.

The coefficients  $P_U^*$  and  $P_L^*$  can be converted into the coefficients  $P_U'$  and  $P_L'$  referred to  $q_1$  (the dynamic pressure in the undisturbed stream) and the corresponding static pressure by means of the following equations, which are based on equations (28) and (40):

$$\left. \begin{aligned} S_U^* &= 1 + \eta - P_U^* \\ S_L^* &= 1 + \eta - P_L^* \\ S_U' &= \frac{q}{q_1} S_U^* = S_U^* \left( 1 + 2 \frac{\Delta \sigma \xi}{\lambda^3} \right) \\ S_L' &= \frac{q}{q_1} S_L^* = S_L^* \left( 1 + 2 \frac{\Delta \sigma \xi}{\lambda^3} \right) \\ P_U' &= 1 + \eta' - S_U' \\ P_L' &= 1 + \eta' - S_L' \end{aligned} \right\} \quad (44)$$

when  $\eta'$  is the value corresponding to  $M'$  given by equation (36).

#### DETERMINATION OF PRESSURE DISTRIBUTION FOR A GIVEN PROFILE SHAPE IN CASCADE

A method can now be outlined for finding the pressure distribution over an airfoil of given profile in an unstaggered cascade. It will be assumed at the outset that the Mach number  $M'$  of the approaching air is known and that the desired lift coefficient  $c_l'$  of each of the cascade airfoils is given.

1. The Mach number of the corresponding free airfoil,  $M$ , is determined from equation (36) to a first order in  $\sigma$  as

$$M = \left( 1 + \frac{\Delta \sigma}{\lambda^3} \mu \right) M' \quad (45)$$

wherein

$$\sigma = \frac{\pi^2}{48} \left( \frac{c}{g} \right)^2 \quad (B11)$$

$$\lambda = \sqrt{1 - (M')^2} \quad (46)$$

$$\mu = 1 + \frac{\gamma - 1}{2} (M')^2 \quad (47)$$

and  $\Delta$  may be obtained from table I or from equation (B20).

2. The lift coefficient of the corresponding free airfoil,  $c_l$ , is found from equation (32) by neglecting second-order terms in  $\sigma$  as

$$c_l = c_l' \left[ 1 + \frac{2\sigma}{\lambda^2} \left( 1 - \frac{\xi}{\lambda} \Delta \right) \right] \quad (48)$$

wherein  $\xi$  is given by equation (29).

For the given airfoil the quarter-chord pitching moment  $c_{m_{c/4}}$  and the angle of attack  $\alpha$  corresponding to the lift coefficient  $c_l$  will be known and the angle of attack for the airfoil in cascade  $\alpha'$  (degrees) can be found from

$$\alpha' = \alpha + 57.3 \frac{\sigma}{\pi \lambda} (c_l + 4c_{m_{c/4}}) \quad (22)$$

3.  $P = P_L - P_U$  for compressible flow at the Mach number  $M$  is found for the single airfoil at the lift coefficient  $c_l$ . Preferably an experimental pressure distribution at the appropriate Mach number and at approximately the same

Reynolds number should be used but a theoretical distribution (e. g., by references 2, 6, 7, or 8) modified by the Glauert-Prandtl or Karman-Tsien rule (references 9 and 10) is satisfactory.

4.  $P^*$  is found from equation (24).

$$P^* = P - \frac{16\sigma c_l}{\pi \lambda^2} \sqrt{\frac{x}{c} \left( 1 - \frac{x}{c} \right)}$$

5.  $\sqrt{1 - P_f^*}$  is calculated from the free airfoil pressure distribution from equations (41) and (42)

$$\sqrt{1 - P_f^*} = \sqrt{1 - P_f} = \frac{\sqrt{1 - P_U} + \sqrt{1 - P_L}}{2} \quad (49)$$

6.  $(1 - P_f^*)$  and  $P^*$  are combined to give  $(1 - P_U^*)$  and  $(1 - P_L^*)$  from equations (43)

$$\left. \begin{aligned} 1 - P_U^* &= \frac{(1 - P_f^* + \frac{1}{4}P^*)^2}{1 - P_f^*} \\ 1 - P_L^* &= \frac{(1 - P_f^* - \frac{1}{4}P^*)^2}{1 - P_f^*} \end{aligned} \right\} \quad (43)$$

7. The cascade pressure coefficients  $P_U'$  and  $P_L'$  are then found by means of equations (44):

$$\left. \begin{aligned} S_U^* &= 1 - P_U^* + \eta \\ S_L^* &= 1 - P_L^* + \eta \\ S_U' &= \left( 1 + 2 \frac{\Delta \sigma \xi}{\lambda^3} \right) S_U^* \\ S_L' &= \left( 1 + 2 \frac{\Delta \sigma \xi}{\lambda^3} \right) S_L^* \\ P_U' &= 1 - S_U' + \eta' \\ P_L' &= 1 - S_L' + \eta' \end{aligned} \right\} \quad (44)$$

where  $\eta$  and  $\eta'$  corresponding to  $M$  and  $M'$ , respectively, are found from figure 2.

#### DETERMINATION OF PROFILE SHAPE FROM A GIVEN PRESSURE DISTRIBUTION IN CASCADE

The procedure for obtaining the profile shape for a given pressure distribution in cascade involves a process which is essentially the reverse of that just outlined. First the required pressure distribution is drawn. The initial choice must be made skillfully with reliance on experimental pressure distributions so that the distribution chosen shall correspond or nearly correspond to that obtainable with a real airfoil. From the chosen distribution the coefficients  $c_l'$  and  $c_{m_{c/4}}'$  are determined by graphical or numerical integration and the pressure coefficients  $P_U'$  and  $P_L'$  are read off at selected points. The method then consists of the following steps:

1. The Mach number  $M$  is determined from

$$M = \left( 1 + \frac{\Delta \sigma}{\lambda^3} \mu \right) M' \quad (45)$$

2.  $P_v^*$  and  $P_L^*$  are found by applying equations (44) in reverse order, neglecting terms involving  $\sigma$  to the second and higher powers.

$$\left. \begin{aligned} S_v' &= 1 + \eta' - P_v' \\ S_L' &= 1 + \eta' - P_L' \\ S_v^* &= \left(1 - 2 \frac{\Delta \sigma \xi}{\lambda^3}\right) S_v' \\ S_L^* &= \left(1 - 2 \frac{\Delta \sigma \xi}{\lambda^3}\right) S_L' \\ P_v^* &= 1 + \eta - S_v^* \\ P_L^* &= 1 + \eta - S_L^* \end{aligned} \right\} \quad (50)$$

where  $\eta'$  and  $\eta$  correspond to  $M'$  and  $M$ . (See fig. 2.)

3.  $(1 - P_f)$  is found by means of the following equations, which are readily obtained from equations (49):

$$\sqrt{1 - P_f} = \sqrt{1 - P_f^*} = \frac{\sqrt{1 - P_v^*} + \sqrt{1 - P_L^*}}{2} \quad (49)$$

The base profile should now be checked to see if it satisfies the closing condition given in reference 2. If the assumed pressure distribution does not correspond to a closed shape, it must be modified so that it does. (See reference 2.)

4. The single-airfoil lift-distribution coefficient  $P$  is found from the relations

$$P^* = P_L^* - P_v^* \quad (51)$$

$$P = P^* + \frac{16\sigma c_i'}{\pi \lambda^2} \sqrt{\frac{x}{c}} \left(1 - \frac{x}{c}\right) \quad (52)$$

5. The final upper- and lower-pressure coefficients are calculated by means of the following equations from equation (43):

$$\left. \begin{aligned} P_v &= 1 - \frac{\left(1 - P_f + \frac{1}{4} P\right)^2}{1 - P_f} \\ P_L &= 1 - \frac{\left(1 - P_f - \frac{1}{4} P\right)^2}{1 - P_f} \end{aligned} \right\} \quad (53)$$

6. The angle of attack of the single airfoil is then given in degrees by

$$\alpha = \alpha' - 57.3 \frac{\sigma}{\pi \lambda} (c_i' + 4c_{m_{c_i'}}) \quad (54)$$

which is a modification of equation (22).

7. The problem of finding a profile shape which will have a given pressure distribution in cascade has now been reduced to the analogous problem for a single airfoil. It is now possible to calculate the corresponding incompressible-flow pressure distribution by the method of reference 10, or simply by multiplying  $P_v$  and  $P_L$  by  $\sqrt{1 - M^2}$ . An airfoil shape can be designed to give this pressure distribution by the method of reference 2. In the application of this method, it is generally necessary to make some changes in the pressure distribution, as previously noted, in order to make it correspond to a possible distribution for an actual airfoil. If the initial distribution has been well chosen, however, the changes will be minor.

#### THE CHOKING OF CASCADES

In the compressible adiabatic flow of a fluid in an elementary stream tube of varying area  $A_i$ , the mass flow must be constant so that the logarithmic derivative

$$\frac{d\rho_i}{\rho_i} + \frac{dV_i}{V_i} + \frac{dA_i}{A_i}$$

must vanish. Now the density  $\rho_i$  and the velocity  $V_i$  are related to the pressure  $p_i$  by Bernoulli's equation.

$$\frac{dp_i}{\rho_i} = \frac{dp_i}{d\rho_i} \times \frac{d\rho_i}{\rho_i} = -V_i dV_i$$

The quantity  $dp_i/d\rho_i$  is, of course, the square of the velocity of sound so that Bernoulli's equation may be written

$$\frac{d\rho_i}{\rho_i} = -\frac{V_i dV_i}{a_i^2} = -M_i^2 \frac{dV_i}{V_i}$$

where  $M_i$  is the local Mach number. Combining this expression with that of the logarithmic derivative then

$$(1 - M_i^2) \frac{dV_i}{V_i} = -\frac{dA_i}{A_i}$$

From this relation it is seen that for a subsonic flow the area must decrease for a velocity increase, while at supersonic speeds the area must increase for a velocity increase. When the Mach number is unity, then  $dA = 0$ , so that sound speed is only attained where the area is a minimum.

Considering the flow through the cascade of figure 1 as essentially unidimensional, then it is apparent that if the flow past the plane  $bb$  attains sonic speed, the mass flow through the cascade cannot be further increased and the cascade flow may be said to be "choked." Of course, the flow through a cascade is not unidimensional, but experience with the similar phenomena of choking in wind tunnels has indicated that the assumption of unidimensionality of flow yields calculated choking Mach numbers in good agreement with experiment.

For a unidimensional flow it is shown in reference 3 that the ratio of the free area of the undisturbed stream  $A$  to the minimum flow area  $A_m$  is related to the choking Mach number of the free stream  $M_{ch}$  by

$$\frac{A}{A_m} = \frac{1}{M_{ch}} \left[ 1 + \frac{\gamma - 1}{\gamma + 1} (M_{ch}^2 - 1) \right]^{\frac{\gamma + 1}{2(\gamma - 1)}} \quad (55)$$

For the approaching stream which will pass between any two airfoils of the cascades the free cross-sectional area is

$$A = g \cos \alpha'$$

while the minimum area between the two airfoils is

$$A_m = g - t = g \left(1 - \frac{t}{g}\right)$$

and hence

$$\frac{A}{A_m} = \frac{\cos \alpha'}{1 - \frac{t}{g}} \quad (56)$$

where  $t$  is the maximum thickness of an airfoil.

Properly the thickness of the boundary layers on each surface of the airfoil should be added to the geometric thickness to obtain an effective thickness  $t_e$ . Using this value with equations (55) and (56) and a value of  $\gamma$  (for air) of 1.4 then

$$\frac{t_e}{g} = 1 - \frac{M_{ch} \cos \alpha'}{\left(\frac{5 + M_{ch}^2}{6}\right)^3} \quad (57)$$

A practical estimate of the choking Mach number may be found by assuming the angle of attack to be so small that  $\cos \alpha' \cong 1$  and that the effective thickness is the geometric thickness. With these assumptions, values of the thickness/gap ratio as a function of the choking Mach number are given in figure 3.

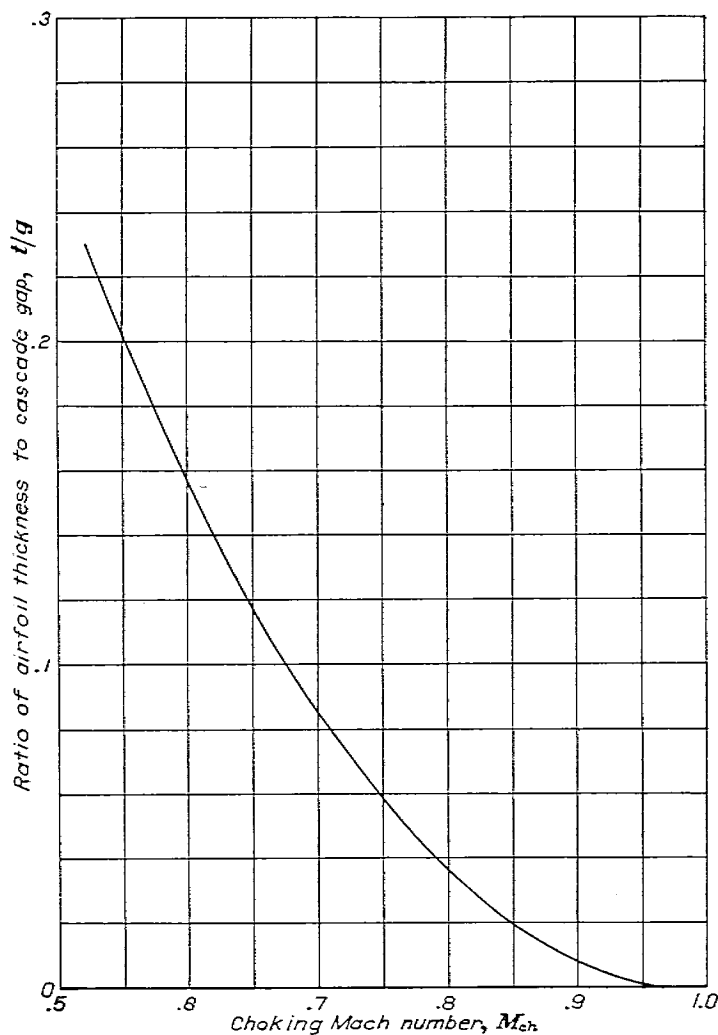


FIGURE 3.—Choking Mach number as a function of the ratio of airfoil thickness to cascade gap.

It is shown in reference 3 that there exists another possibility that choking may occur in the wake of the airfoils for very thin profiles as the result of the action of viscosity. In most cases this type of choking will not be of practical importance.

## DISCUSSION

In order to check the accuracy of the equations which have been developed, pressure distributions for incompressible flow have been calculated at three lift coefficients for an unstaggered cascade of NACA 4412 airfoils. These cases were chosen to permit comparison with those which have been determined in reference 11 by the method of conformal transformation. The chord/gap ratio in all cases is 1.03 and the lift coefficients considered are 0, 0.5, and 1.0. This comparison subjects the approximate theory of this report to a rather severe test, since the analysis has been developed on the basis of a small chord/gap ratio. The comparison with reference 11 indicates the agreement is good as may be seen in figures 4, 5, and 6. The single-airfoil pressure distributions, as obtained by conformal transformation in reference 11, are shown in the figures for the same lift coefficients as for the cascade airfoils. (In Appendix C the calculations to obtain the pressure distribution of figure

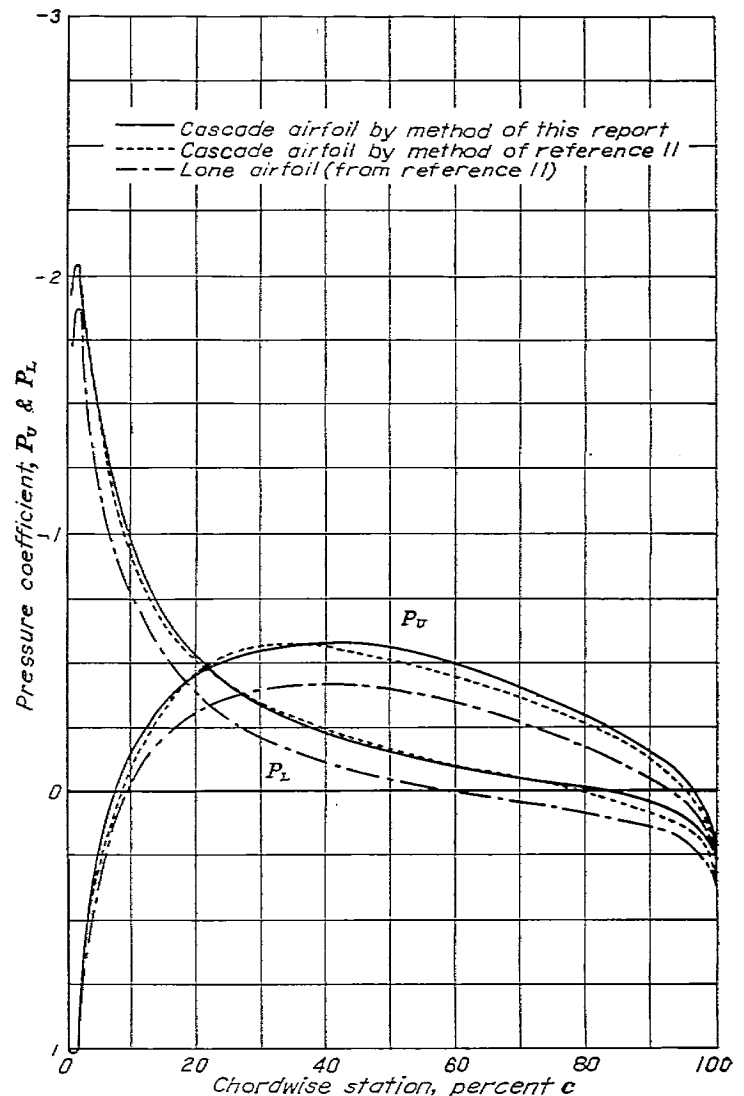


FIGURE 4.—Pressure distribution for NACA 4412 airfoil alone and in cascade for  $\frac{c}{g}=1.03$  and  $\alpha'=0$ .

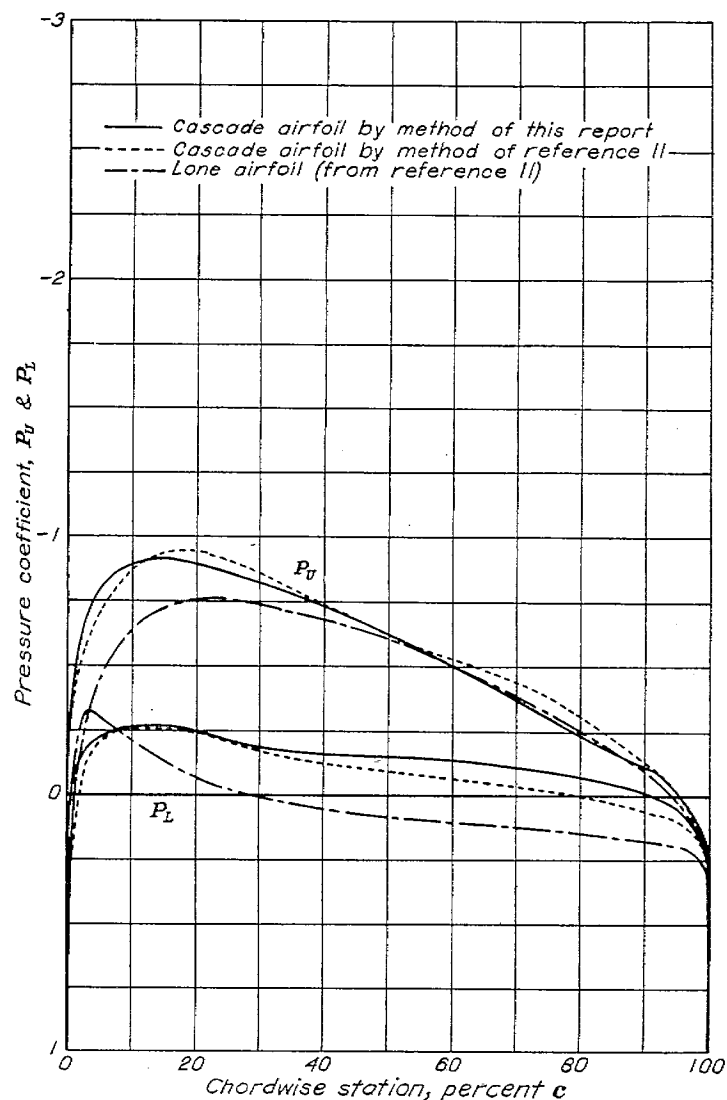


FIGURE 5.—Pressure distribution for NACA 4412 airfoil alone and in cascade for  $\frac{c}{g}=1.03$  and  $c_t'=0.5$ .

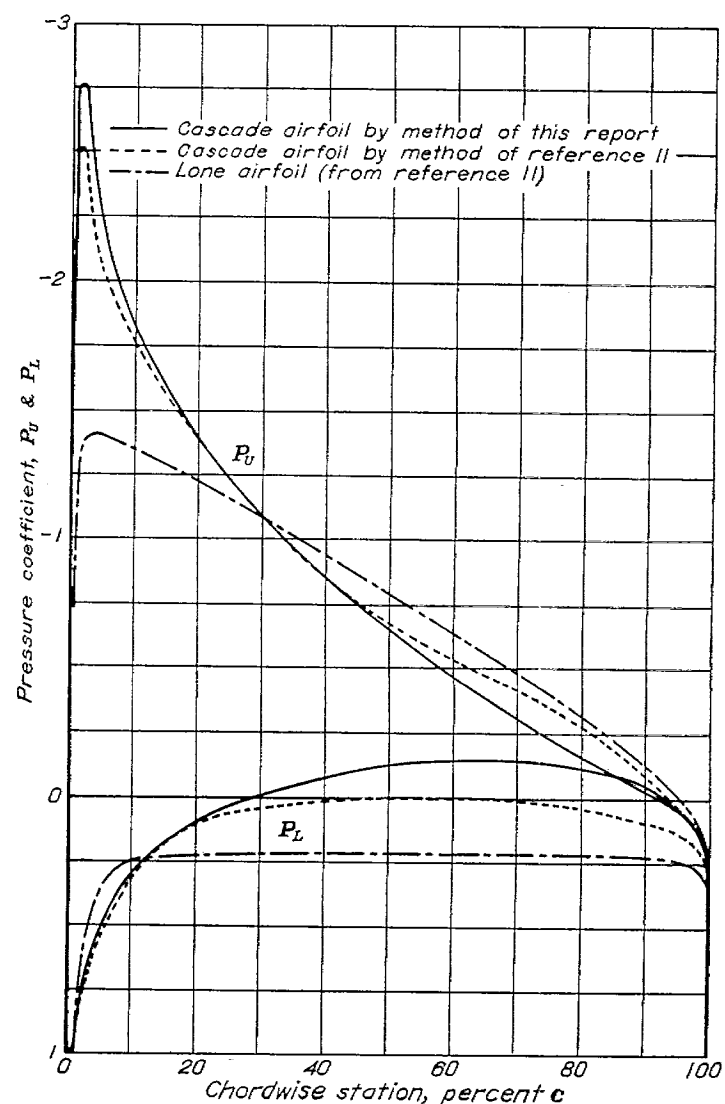


FIGURE 6.—Pressure distribution for NACA 4412 airfoil alone and in cascade for  $\frac{c}{g}=1.03$  and  $c_t'=1.0$ .

6 are given in detail. Table II gives all the necessary computations and serves to demonstrate the simplicity of the method.) It is evident from the figures that one effect of cascading airfoils is to impose a "negative camber influence" on the pressure distributions as the lift coefficient is increased. Accordingly, for airfoils for use in cascade the camber must be exaggerated if a certain desired camber effect on the pressure distribution is to be obtained. It is of interest to note that the calculated angles of attack are also in reasonably good agreement as may be seen in the following tabulation:

$c_t'$	Airfoil in cascade		Airfoil alone
	$\alpha'$ (from reference 11)	$\alpha'$ (method of report)	$\alpha$
0	-5.9°	-6.0°	-4.3°
.5	+1.8°	+2.3°	-1.1°
1.0	+9.7°	+10.4°	+4.0°

Unfortunately no pressure distributions over unstaggered cascades at high airspeeds could be found so that the validity of the compressibility corrections developed in this report could not be determined. They have been developed, however, in much the same way as the compressibility corrections of reference 3, which have been found to be in good agreement with experiment. It is clear, however, that as the Mach number is increased the accuracy of the calculations will diminish unless the chord/gap ratio is simultaneously decreased. This will be particularly true as the choking Mach number is approached.

One matter of interest concerns the effect of compressibility on the lift-curve slope of a cascade of NACA 4412 airfoils having chord/gap ratios of 0 (i. e., lone airfoil), 0.5, and 1.0 which is shown in figure 7. It is seen that the importance of the interference effects of the airfoils in cascade increase so rapidly with Mach number that, contrary to the usual expectation, a decrease in lift-curve slope with Mach number is indicated for high solidities.

An examination of the equations for the choking of cascades indicates that care must be exercised with an unstaggered cascade to keep the airfoil thickness small for high



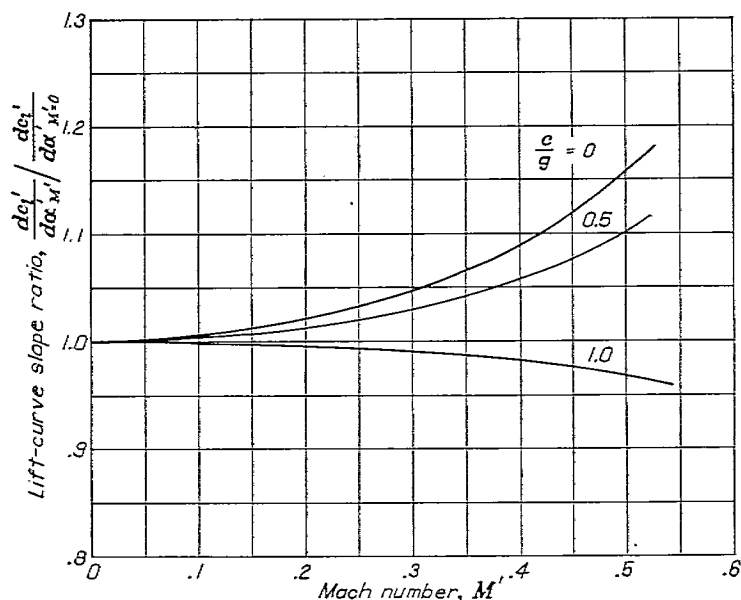


FIGURE 7.—Effect of compressibility on lift-curve slope for NACA 4412 airfoil in cascade.

solidities if relatively high free-stream Mach numbers are employed. Even for the cascade considered in figures 4, 5, and 6, for example, the choking Mach number as obtained from figure 3 is only about 0.64 based on the geometric thickness of the airfoils.

The existence of a boundary layer on the airfoil surfaces would, of course, increase the effective thickness which would reduce the choking Mach number. When the pressure gradients are strongly adverse, as in the case of the airfoil of figure 6, the boundary-layer growth will be increased and its effect on the choking Mach number will be more pronounced. The proper choice of camber consistent with the design lift will serve to reduce the sharp pressure peak, thereby improving the critical as well as the choking Mach number.

AMES AERONAUTICAL LABORATORY,  
NATIONAL ADVISORY COMMITTEE FOR AERONAUTICS,  
MOFFETT FIELD, CALIF., September, 1947.

## APPENDIX A

### LIST OF SYMBOLS

The following symbols are used through this report:

$a$	velocity of sound
$A_n$	Fourier coefficients (See equation (7).)
$B_n$	Fourier coefficients (See equation (B14).)
$c$	airfoil chord
$c_l$	section lift coefficient
$c_{m_{c/4}}$	section quarter-chord-moment coefficient
$g$	distance perpendicular to chord between airfoils in cascade
$H$	total head
$L$	lift per unit span
$M$	Mach number
$M_{ch}$	choking Mach number
$p$	static pressure
$P$	without subscript, local lift at any chord station in coefficient form; with subscript, local pressure coefficient (See equation (38).)
$q$	dynamic pressure
$Q$	source strength
$r$	radial distance in polar coordinates
$S$	local pressure coefficient (See equation (38).)
$t$	maximum airfoil thickness
$T$	absolute temperature
$u$	horizontal component of velocity
$v$	vertical component of velocity
$\Delta v$	total induced vertical velocity at the airfoil under consideration due to the other airfoils in the cascade
$V$	velocity
$x$	coordinate of points on chord line as measured from leading edge
$y_c$	ordinate of mean camber line
$y_t$	ordinate of base profile
$\alpha$	angle of attack

$\gamma$	ratio of specific heat at constant pressure to specific heat at constant volume ( $c_p/c_v$ )
$\Gamma$	circulation per unit span
$\xi$	compressibility correction factor $\left(1 - \frac{M^2}{2}\right)$
$\eta$	compressibility factor (See equation (39) and fig. 2.)
$\theta$	angular coordinate of points on chord line (See equation (7).)
$\lambda$	compressibility correction factor ( $\sqrt{1-M^2}$ )
$\Lambda$	factor depending upon shape of base profile (See equation (B20) and table I.)
$\mu$	compressibility correction factor $\left(1 + \frac{\gamma-1}{2} M^2\right)$
$\rho$	mass density
$\sigma$	factor depending upon solidity of cascade $\left(\frac{\pi^2}{48} \frac{c^2}{g^2}\right)$
$\tau$	inclination of the radius $r$ to a line normal to the airfoil chord (See fig. 1.)
$\Phi$	polar angle in polar coordinates (positive counter-clockwise)

### SUPERSCRIPTS

'	used to distinguish properties of cascade airfoil
*	denotes cascade airfoil characteristics as coefficients referred to dynamic pressure of incident stream at center of pressure

### SUBSCRIPTS

<sup>1</sup>	denotes values in stream far ahead of cascade (except when used to indicate a numbered Fourier coefficient)
$l$	denotes local conditions at point in fluid
$L$	denotes values on lower surface of airfoil
$U$	denotes values on upper surface of airfoil
$f$	refers to base profile
$v$	denotes a velocity induced by a vortex
$s$	denotes a velocity induced by a source or sink

## APPENDIX B

### VELOCITY COMPONENTS INDUCED BY AIRFOILS IN CASCADE

For incompressible flow over a single airfoil, the vertical velocity (perpendicular to the chord) induced at the point on the chord  $x_0$  by its own vorticity distribution is

$$v = \frac{1}{2\pi} \int_0^c \frac{d\Gamma}{dx} \frac{dx}{x-x_0} \quad (\text{B1})$$

To obtain the velocity for compressible flow, the factor

$$\frac{\sqrt{1-M^2}}{1-M^2 \sin^2 \Phi} \quad (\text{B2})$$

must be applied to the right-hand side of equation (B1) as is shown in reference 9. Here  $M$  is the Mach number of the undisturbed stream and  $\Phi$  is the angle between the stream direction and a line drawn from the vortex to the point in question. For a single airfoil  $\Phi$  is always close to  $0^\circ$  or  $180^\circ$  and the induced velocity in a compressible stream is approximately

$$v = \frac{\sqrt{1-M^2}}{2\pi} \int_0^c \frac{d\Gamma}{dx} \frac{dx}{x-x_0} = \frac{\lambda}{2\pi} \int_0^c \frac{d\Gamma}{dx} \frac{dx}{x-x_0} \quad (\text{B3})$$

where

$$\lambda = \sqrt{1-M^2} \quad (\text{B4})$$

Equation (B3) can be integrated by substituting for  $d\Gamma/dx$  and for  $x$  the following:

$$\frac{d\Gamma}{dx} = 2V \left( A_0 \cot \frac{1}{2}\theta + \sum_{n=1}^{\infty} A_n \sin n\theta \right) \quad (6)$$

$$x = \frac{c}{2} (1 - \cos \theta) \quad (7)$$

The details of the integration are given in reference 2, page 4. The resulting expression is

$$\frac{v}{V} = \lambda \left( -A_0 + \sum_{n=1}^{\infty} A_n \cos n\theta \right) \quad (\text{B5})$$

The vertical velocity at a point on the chord of an airfoil in cascade is made up of three parts. These are (1) the velocity  $v'$  induced by its own vortices, (2) the velocity  $\Delta v_s$  induced by the vortices of the remaining airfoils of the cascade, and (3) the velocity  $\Delta v_s$  induced by the sources and sinks of the remaining airfoils.

By analogy with equation (B5):

$$\frac{v'}{V} = \lambda \left( -A_0' + \sum_{n=1}^{\infty} A_n' \cos n\theta \right) \quad (\text{B6})$$

The vertical velocity induced by the vorticity distribution of the other airfoils is given by the expression

$$\Delta v_s = \frac{1}{\pi} \sum_{m=1}^{\infty} \int_0^c \frac{d\Gamma'}{dx} \frac{\sin \tau_m}{r_m} \left( \frac{\sqrt{1-M^2}}{1-M^2 \cos^2 \tau_m} \right) dx \quad (\text{B7})$$

The summation is over the remaining airfoils of the cascade. The angle  $\tau$  is measured clockwise between the vertical and

a line from the vortex to the point in question, as indicated in figure 1. The factor in parentheses is that necessary to give the correct result for compressible flow. It is derived from the factor (B2) with use of the relation  $\sin \Phi = -\cos \tau$ . Since  $r_m = (mg/\cos \tau_m)$  and  $\tan \tau_m = (x-x_0)/mg$  so that

$$\sin \tau_m = \frac{\frac{x-x_0}{mg}}{\sqrt{1+\left(\frac{x-x_0}{mg}\right)^2}}$$

and

$$\cos \tau_m = \frac{1}{\sqrt{1+\left(\frac{x-x_0}{mg}\right)^2}}$$

the preceding equation may be written

$$\Delta v_s = \frac{\lambda}{\pi} \sum_{m=1}^{\infty} \int_0^c \frac{d\Gamma'/dx}{mg} \left[ \frac{\frac{x-x_0}{mg}}{1-M^2+\left(\frac{x-x_0}{mg}\right)^2} \right] dx \quad (\text{B8})$$

Expanding the term in brackets in a power series in  $(x-x_0)/mg$ , neglecting terms involving the cube and higher powers, and noting that

$$\sum_{m=1}^{\infty} \frac{1}{m^2} = \frac{\pi^2}{6}$$

there is obtained

$$\Delta v_s = \frac{\pi}{6\lambda g^2} \int_0^c \frac{d\Gamma'}{dx} (x-x_0) dx \quad (\text{B9})$$

If equations (6) and (7) are substituted into equation (B9) and the indicated integration is performed, there is finally obtained

$$\frac{\Delta v_s}{V} = -2 \frac{\sigma}{\lambda} \left[ (A_0' + \frac{1}{2} A_2') - (2A_0' + A_1') \cos \theta \right] \quad (\text{B10})$$

where

$$\sigma = \frac{\pi^2}{48} \frac{c^2}{g^2} \quad (\text{B11})$$

It is interesting to note that equation (B10) can be more directly obtained by replacing each of the airfoils of the cascade by a single vortex. The important point in such a derivation is the proper chordwise location of this vortex at the airfoil center of pressure.

In a manner similar to that in which equation (B10) was obtained it is possible to show that neglecting terms involving  $(x-x_0)/mg$  to the third and higher powers,

$$\frac{\Delta u_s}{V} = 0 \quad (\text{B12})$$

In Appendix B of reference 3 the velocity components induced by a source at the origin are given as follows: The velocity component perpendicular to the stream  $\Delta v_s$  is

$$\frac{Q}{2\pi r} \left[ \frac{\sqrt{1-M^2} (\sin \Phi)}{1-M^2 \sin^2 \Phi} \right]$$

and the induced velocity component parallel to the stream  $\Delta u_s$  is

$$\frac{Q}{2\pi r} \left[ \frac{\cos \Phi}{\sqrt{1-M^2} (1-M^2 \sin^2 \Phi)} \right]$$

where  $Q$  is the mass flow divided by the free-stream density.

The vertical velocity induced by the source-sink distributions of the remaining airfoils of the cascade can then be expressed as

$$\Delta v_s = -\frac{1}{\pi} \sum_{m=1}^{\infty} \int_0^c \frac{dQ'/dx}{r_m} \left[ \frac{\sqrt{1-M^2} (\cos \tau_m)}{1-M^2 \cos^2 \tau_m} \right] dx$$

and the corresponding horizontal induced velocity is, after noting that  $\cos \Phi = -\sin \tau_m$ ,

$$\Delta u_s = -\frac{1}{\pi} \sum_{m=1}^{\infty} \int_0^c \frac{dQ'/dx}{r_m} \left[ \frac{\sin \tau_m}{\sqrt{1-M^2} (1-M^2 \cos^2 \tau_m)} \right] dx$$

where  $\frac{dQ'}{dx} dx$  is the source strength over an element of chord  $dx$  of the cascade airfoil. Substituting for  $r_m$  and  $\cos \tau_m$  and  $\sin \tau_m$  as before, expanding, and neglecting the third and higher power of  $(x-x_0)/mg$ , there is obtained

$$\left. \begin{aligned} \Delta v_s &= 0 \\ \Delta u_s &= -\frac{\pi}{6\lambda^3 g^2} \int_0^c \frac{dQ'}{dx} (x-x_0) dx \end{aligned} \right\} \quad (B13)$$

The source-sink distribution  $\frac{dQ'}{dx}$  is now expressed by the following series:

$$\frac{dQ'}{dx} = 2V(B_0' \cot \frac{1}{2} \theta + \sum_{n=1}^{\infty} B_n' \sin n\theta) \quad (B14)$$

On substitution of equation (B14) the integral in equation (B13) can be evaluated, obtaining, analogously with equations (B10) and (B12):

$$\frac{\Delta v_s}{V} = 0 \quad (B15)$$

and

$$\frac{\Delta u_s}{V} = \frac{2\sigma}{\lambda^3} [(B_0' + \frac{1}{2} B_2') - (2B_0' + B_1') \cos \theta] \quad (B16)$$

Since the airfoil must be a closed figure, it follows that

$$\int_0^c \frac{dQ'}{dx} dx = 0 \quad (B17)$$

By substitution of equation (B14) in equation (B17), there is obtained

$$2B_0' + B_1' = 0 \quad (B18)$$

so that

$$\frac{\Delta u_s}{V} = \frac{\sigma}{\lambda^3} (2B_0' + B_2')$$

From thin airfoil theory (reference 2) it can be shown that

$$2B_0' + B_2' = \frac{16}{\pi} \int_0^1 \frac{y_t}{c} d\left(\frac{x}{c}\right) \quad (B19)$$

where  $y_t$  is the ordinate of the base profile as measured from the axis of symmetry in terms of the airfoil chord at the corresponding  $x$  station.

In the problem of determining the wall interference in a two-dimensional wind tunnel, an evaluation of the influence of the image base profiles yields an identical result if the limitations of thin airfoil theory are presumed. Lock (discussed in reference 3) has evaluated the image base profile effects as regards wall interference in the incompressible case for profiles not necessarily thin and has found that (in the notation of this report)

$$\Lambda = \frac{16}{\pi} \int_0^1 \frac{y_t}{c} \sqrt{(1-P_t) \left[ 1 + \left( \frac{dy_t}{dx} \right)^2 \right]} d\left(\frac{x}{c}\right) \quad (B20)$$

is a more precise value to replace  $2B_0' + B_2'$ , where  $P_t$  is the base-profile pressure coefficient in incompressible flow. Values of  $\Lambda$  computed by equation (B20) for various airfoils are given in table I which was taken from reference 3. Accordingly, as in reference 3, this value is used in this report so that the velocity increment due to the effect of sources and sinks becomes

$$\frac{\Delta u_s}{V} = \frac{\Lambda \sigma}{\lambda^3} \quad (B21)$$

It should be noted that properly Lock's result for incompressible flow is

$$\frac{\Delta u_s}{V_1} = \Lambda \sigma \quad (B22)$$

However, the expression for  $V$  is

$$V = V_1 + \Delta u$$

so it follows that

$$\frac{V_1}{V} = 1 - \frac{\Delta u}{V}$$

Thus for incompressible flow

$$\frac{\Delta u_s}{V} = \Lambda \sigma \left( 1 - \frac{\Delta u}{V} \right) \quad (B23)$$

which to the first order in  $\sigma$  is still equation (B22) so that equation (B21) for compressible flow follows. From equations (B12) and (B21) it is clear that the influence at the position of one airfoil of the cascade due to all other airfoils of the cascade is simply that promoted by the source-sink system

$$\frac{\Delta u}{V} = \frac{\Lambda \sigma}{\lambda^3} \quad (B24)$$

Moreover, because  $\Delta v_s$  (equation (B13)) is zero, it follows from equation (B10)

$$\frac{\Delta v}{V} = -2 \frac{\sigma}{\lambda} \left[ (A_0' + \frac{1}{2} A_2') - (2A_0' + A_1') \cos \theta \right] \quad (B25)$$

## APPENDIX C

### SAMPLE PRESSURE-DISTRIBUTION CALCULATION

Table II gives all the necessary calculations to arrive at the cascade pressure distribution shown in figure 6. It was desired to obtain the pressure distribution for a cascade of NACA 4412 airfoils given the values  $c_t=1.0$  and  $c/g=1.03$  for comparison with the distribution calculated by the method of conformal transformation given in reference 11.

Since the assumed flow is incompressible, then  $\lambda$ ,  $\mu$ , and  $\xi$  are unity and  $\eta$  and  $\eta'$  are zero. From table I,  $\Lambda$  is 0.237. The parameter  $\sigma$  is 0.220. The lift coefficient for the corresponding airfoil in free air is obtained from equation (48) as 1.335. By potential theory, for the NACA 4412

airfoil the free-air angle of attack for  $c_t=1.335$  is  $6.8^\circ$  and  $c_{m_{c/4}}$  is  $-0.11$  so that for the airfoil in cascade, by equation (22),  $\alpha'=10.4^\circ$ .

Values of the pressure coefficient for the isolated airfoil were calculated from the free-air values of reference 11 using the method of reference 5. From these pressures  $P$  was determined and the  $P^*$  was obtained from equation (24).  $P^*$  and  $1-P_f^*$  (equal to  $1-P_f$ ) were then combined by equations (43) to give  $1-P_u^*$  and  $1-P_L^*$ . The cascade pressure distribution was finally obtained using equations (44).

TABLE I.—VALUES OF  $\Lambda$  FOR VARIOUS BASE PROFILES

$\frac{t}{c}=0.XX$	RANKINE OVAL	ELLIPSE	JOUKOWSKI SECTION	CONVENTIONAL NACA SECTIONS— 00XX	NACA LOW-DRAG SECTIONS												
					07-OXX	10-OXX	18-OXX	19-OXX	27-OXX	35-OXX	45-OXX	63-OXX	64-OXX	65-OXX	66-OXX	67-OXX	
0.06		0.127		0.111	0.125	0.119	0.124	0.127	0.119	0.107	0.106	0.101	0.106	0.109	0.117	0.119	
0.09	0.236	.196	0.155	.172	.190	.183	.189	.195	.185	.159	.157	.145	.153	.163	.174	.178	
0.12	.320	.269	.212	.237	.264	.253	.263	.271	.256	.217	.214	.201	.215	.221	.236	.243	
0.15	.403	.345	.273	.305	.342	.326	.341	.353	.330	.281	.278	.257	.276	.283	.301	.311	
0.18	.493	.425	.337	.376	.425	.404	.424	.439	.405	.348	.344	.316	.338	.348	.368	.379	
0.21	.580	.508	.404	.450	.512	.484	.511	.529	.489	.417	.415	.378	.402	.414	.436	.450	
0.25	.703	.625	.497	.554	.632	.596	.631	.654	.602	.512	.513	.460	.487	.501	.526	.543	
0.30	.864	.780	.626	---	---	---	---	---	---	---	---	---	---	---	---	---	
0.35	1.049	.945	.767	---	---	---	---	---	---	---	---	---	---	---	---	---	
0.50	1.690	1.507	1.258	---	---	---	---	---	---	---	---	---	---	---	---	---	
1.00	4.000	4.000	---	---	---	---	---	---	---	---	---	---	---	---	---	---	

TABLE II.—CALCULATION OF CASCADE PRESSURE DISTRIBUTION OF FIGURE 6 (SEE APPENDIX C)

[ $\sigma=0.220$ ;  $\Lambda=0.237$ ]

①	②	③	④	⑤	⑥	⑦	⑧	⑨	⑩	⑪	⑫	⑬
Station	$P_U$	$P_L$	$P^*=③-④$	$1-P_f^*=\left(\frac{\sqrt{1-⑤}+\sqrt{1-⑥}}{2}\right)$	$\frac{10}{\pi} \arcsin \sqrt{⑥(1-⑤)}$	$P^*=③-⑥$	$S_U^*=\frac{\left(\frac{⑤+⑥}{4}\right)^2}{⑥}$	$S_L^*=\frac{\left(\frac{⑤-⑥}{4}\right)^2}{⑥}$	$S_U'=(1+2\Lambda\sigma)⑩$	$S_L'=(1+2\Lambda\sigma)⑪$	$P_U'=1-⑫$	$P_L'=1-⑬$
0.025	-2.46	0.59	3.35	1.19	0.23	3.12	3.26	0.14	3.60	0.16	-2.60	0.84
0.05	-2.17	.68	2.85	1.37	.33	2.62	2.92	.40	3.23	.44	-2.23	.56
.1	-1.87	.50	2.37	1.44	.45	2.12	2.56	.64	2.83	.71	-1.83	.29
.15	-1.69	.44	2.13	1.43	.53	1.86	2.34	.74	2.58	.82	-1.58	.18
.2	-1.55	.39	1.94	1.41	.60	1.64	2.16	.82	2.39	.90	-1.39	.10
.3	-1.32	.35	1.67	1.35	.68	.99	1.89	.90	2.09	1.00	-1.09	0
.4	-1.12	.33	1.45	1.30	.73	.72	1.68	.96	1.86	1.06	-.86	-.06
.5	-.92	.29	1.21	1.24	.75	.46	1.48	1.02	1.64	1.13	-.64	-.13
.6	-.74	.27	1.01	1.18	.73	.28	1.32	1.04	1.46	1.15	-.46	-.15
.7	-.56	.26	.82	1.11	.68	.14	1.18	1.04	1.30	1.15	-.30	-.15
.8	-.38	.26	.64	1.03	.60	-.04	1.06	1.01	1.17	1.12	-.17	-.12
.9	-.16	.24	.41	.95	.45	-.04	.93	1.01	1.03	1.07	-.03	-.07
1.0	1.00	1.00	0	0	0	0	0	0	0	1.00	1.00	1.00

## REFERENCES

1. Glauert, H.: The Elements of Aerofoil and Airscrew Theory. The University Press, Cambridge, 1926.
2. Allen, H. Julian: General Theory of Airfoil Sections Having Arbitrary Shape or Pressure Distribution. NACA Rep. No. 833, 1943.
3. Allen, H. Julian, and Vincenti, Walter G.: Wall Interference in a Two-Dimensional-Flow Wind Tunnel with Consideration of the Effect of Compressibility. NACA Rep. No. 782, 1944.
4. Stack, John: The N. A. C. A. High-Speed Wind Tunnel and Tests of Six Propeller Sections. NACA Rep. No. 463, 1933.
5. Allen, H. Julian: A Simplified Method for the Calculation of Airfoil Pressure Distribution. NACA TN No. 708, 1939.
6. Theodorsen, Theodore: Theory of Wing Sections of Arbitrary Shape. NACA Rep. No. 411, 1931.
7. Jacobs, Eastman N., and Rhode, R. V.: Airfoil Section Characteristics as Applied to the Prediction of Air Forces and Their Distribution on Wings. NACA Rep. No. 631, 1938.
8. Abbott, Ira H., von Doenhoff, Albert E., and Stivers, Louis S., Jr.: Summary of Airfoil Data. NACA Rep. No. 824, 1945.
9. Glauert, H.: The Effect of Compressibility on the Lift of an Aerofoil. R. & M. No. 1135, British A. R. C., 1927.
10. von Kármán, Th.: Compressibility Effects in Aerodynamics. Jour. Aero. Sci., vol. 8, no. 9, July 1941, pp. 337-356.
11. Garrick, I. E.: On the Plane Potential Flow Past a Symmetrical Lattice of Arbitrary Airfoils. NACA Rep. No. 788, 1944.